

Modelling and Co-ordination Control of Hybrid Grid

S. Lakshmi Devi*

M. Tech. (PE) EEE & JNTU Kakinada

K. Sudheer

Assoc. Prof. in EEE & JNTU Kakinada

Abstract

This project proposes a hybrid ac/dc micro grid to reduce the processes of multiple dc-ac-dc or ac-dc-ac conversions in an individual ac or dc grid. The hybrid grid consists of both ac and dc networks connected together by multi-bidirectional converters. AC sources and loads are connected to the ac network whereas dc sources and loads are tied to the dc network. Energy storage systems can be connected to dc or ac links. The proposed hybrid grid can operate in a grid-tied or autonomous mode. The coordination control algorithms are proposed for smooth power transfer between ac and dc links and for stable system operation under various generation and load conditions. Uncertainty and intermittent characteristics of wind speed, solar irradiation level, ambient temperature, and load are also considered in system control and operation. A small hybrid grid has been modeled and simulated using the Simulink in the MATLAB. The simulation results show that the system can maintain stable operation under the proposed coordination control schemes when the grid is switched from one operating condition to another

Index Terms

Energy management, grid control, grid operation, hybrid micro grid, PV system, wind power generation.

1. INTRODUCTION

Three phase ac power systems have existed for over 100 years due to their efficient transformation of ac power at different voltage levels and over long distance as well as the inherent characteristic from fossil energy driven rotating machines. Recently more renewable power conversion systems are connected in low voltage ac distribution systems as distributed generators or ac micro grids due to environmental issues caused by conventional fossil fueled power plants. On other hand, more and more dc loads such as light-emitting diode (LED) light sand electric vehicles (EVs) are connected to ac power systems to save energy and reduce CO emission. When power can be fully supplied by local renewable power sources, long distance high voltage transmission is no longer necessary. AC micro grids have been proposed to facilitate the connection of renewable power sources to conventional ac systems. However, dc power from photovoltaic (PV) panels or fuel cells has to be converted into ac using dc/dc boosters and dc/ac inverters in order to connect to an ac grid.

Recently, dc grids are resurging due to the development and deployment of renewable dc power sources and their inherent advantage for dc loads in commercial, industrial

and residential applications. The dc micro grid has been proposed to integrate various distributed generators. However, ac sources have to be converted into dc before connected to a dc grid and dc/ac inverters are required for conventional ac loads. Multiple reverse conversions required in individual ac or dc grids may add additional loss to the system operation and will make the current home and office appliances more complicated.

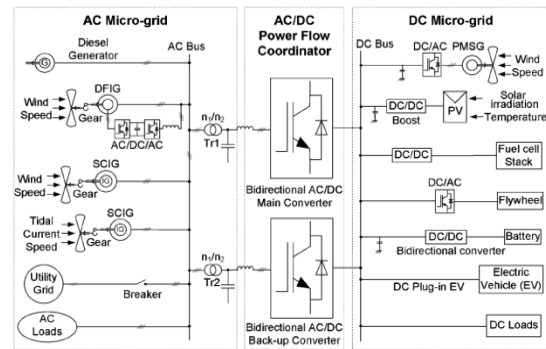


Figure1 hybrid ac/dc micro grid system

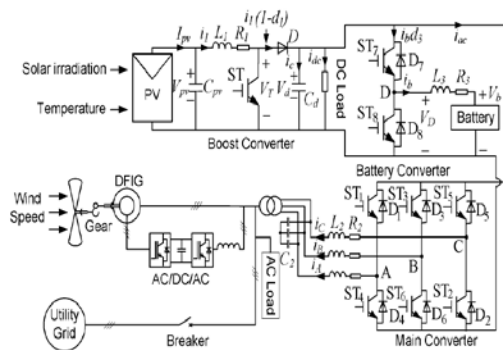


Figure 2 proposed hybrid grid compact representation

A hybrid ac/dc micro grid is proposed in this project to reduce processes of multiple reverse conversions in an individual ac or dc grid and to facilitate the connection of various renewable ac and dc sources and loads to power system. Since energy management, control, and operation of a hybrid grid are more complicated than those of an individual ac or dc grid, different operating modes of a hybrid ac/dc grid have been investigated. The coordination control schemes among various converters have been

proposed to harness maximum power from renewable power sources, to minimize power transfer between ac and dc networks, and to maintain the stable operation of both ac and dc grids under variable supply and demand conditions when the hybrid grid operates in both grid-tied and islanding modes. The advanced power electronics and control technologies used in this project will make a future power grid much smarter.

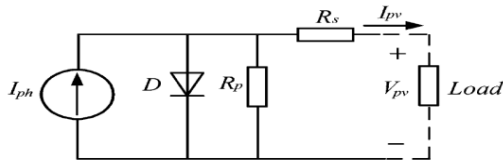


Fig .3 Equivalent circuit of a solar cell.

Symbol	Description	Value
V_{oc}	Rated open circuit voltage	403V
I_{ph}	Photo current	
I_{sat}	Module reverse saturation current	
q	Electron charge	$1.602 \times 10^{-19} C$
A	Ideality factor	1.50
k	Boltzmann constant	$1.38 \times 10^{-23} J/k$
R_s	Series resistance of PV cell	
R_p	Parallel resistance of PV cell	
I_{SSO}	Short circuit current	3.27A
k_i	SC current temperature coefficient	$1.7e^{-3}$
T_r	Reference temperature	301.18K
I_{rr}	Reverse saturation current at T_r	$2.0793e^{-6} A$
E_{gap}	Energy of the band gap for silicon	1.1eV
n_p	Number of cells in parallel	40
n_s	Number of cells in series	900
S	Solar radiation level	$0 \sim 1000 W/m^2$
T	Surface temperature of PV	350 K

Table 1 parameters for photovoltaic panel

2. SYSTEM CONFIGURATION AND MODELING

A Grid configuration

The figure 1 shows a conceptual hybrid system configuration where various ac and dc sources and loads are connected to the corresponding dc and ac networks. The ac and dc links are connected together through two transformers and two four-quadrant operating three phase converters. The ac bus of the hybrid grid is tied to the

utility grid. A compact hybrid grid as shown in Fig. 2 is modeled using the Simulink in the MATLAB to simulate system operations and controls. Forty kW PV arrays are connected to dc bus through a dc/dc boost converter to simulate dc sources.

A capacitor is to suppress high frequency ripples of the PV output voltage. A 50 kW wind turbine generator (WTG) with doubly fed induction generator (DFIG) is connected to an ac bus to simulate ac sources. A 65 Ah battery as energy storage is connected to dc bus through a bidirectional dc/dc converter. Variable dc load (20 kW–40 kW) and ac load (20 kW–40 kW) are connected to dc and ac buses respectively. The rated voltages for dc and ac buses are 400 V and 400 V rms respectively. A three phase bidirectional dc/ac main converter with R-L-C filter connects the dc bus to the ac bus through an isolation transformer.

B Grid operation

The hybrid grid can operate in two modes. In grid-tied mode, the main converter is to provide stable dc bus voltage and required reactive power and to exchange power between the ac and dc buses. The boost converter and WTG are controlled to provide the maximum power.

When the output power of the dc sources is greater than the dc loads, the converter acts as an inverter and injects power from dc to ac side. When the total power generation is less than the total load at the dc side, the converter injects power from the ac to dc side. When the total power generation is greater than the total load in the hybrid grid, it will inject power to the utility grid. Otherwise, the hybrid grid will receive power from the utility grid. In the grid tied mode, the battery converter is not very important in system operation because power is balanced by the utility grid. In autonomous mode, the battery plays a very important role for both power balance and voltage stability. Control objectives for various converters are dispatched by energy management system. DC bus voltage is maintained stable by a battery converter or boost converter according to different operating conditions. The main converter is controlled to provide a stable and high quality ac bus voltage. Both PV and WTG can operate on maximum power point tracking (MPPT) or off-MPPT mode based on system operating requirements. Variable wind speed and solar irradiation applied to the WTG and PV arrays respectively to simulate variation of power of ac and dc sources and test the MPPT control algorithm.

C Modeling of PV Panel

The above Fig.3 shows the equivalent circuit of a PV panel with a load. The current output of the PV panel is modeled by the following three equations. All the parameters are shown in table 1

$$I_{pv} = n_p I_{ph} - n_p I_{sat} \times \left[\exp\left(\frac{q}{AKT}\right) \left(\frac{V_{pv}}{n_s} + I_{pv} R_s\right) - 1 \right] \quad 1$$

$$I_{ph} = (I_{sso} + K_i(T - T_r)) \cdot \frac{S}{1000} \quad 2$$

$$I_{sat} = I_{rr} \left(\frac{T}{T_r}\right)^3 \exp\left(\left(\frac{qE_{gap}}{kA}\right) \cdot \left(\frac{1}{T_r} - \frac{1}{T}\right)\right) \quad 3$$

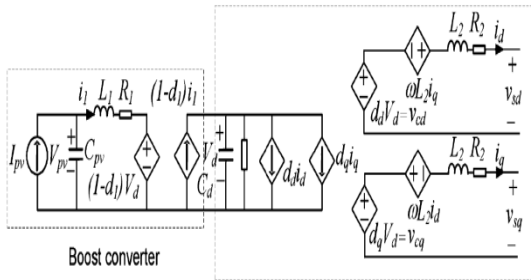


Fig. 4 Time average model for the booster and main converter.

D Modeling of Battery:

Two important parameters to represent state of a battery are terminal voltage v_b and state of charge (SOC) as follows

$$V_b = V_0 + R_b \cdot i_b - K \frac{Q}{Q + \int i_b dt} + A \cdot \exp\left(B \int i_b dt\right) \quad 4$$

$$SOC = 100 \left(1 + \frac{\int i_b dt}{Q}\right) \quad 5$$

Where R_b is internal resistance of the battery, V_0 is the open circuit voltage of the battery, i_b is battery charging current, K is polarization voltage, Q is battery capacity, A is exponential voltage, B and is exponential capacity

E Modeling of Wind Turbine Generator:

Power output P_m from a WTG is determined by

$$P_m = 0.5 \rho A C_p(\lambda, \beta) V_\omega^3 \quad 6$$

Where ρ is air density, A is rotor swept area, V_ω is wind speed, and $C_p(\lambda, \beta)$ is the power coefficient, which is the function of tip speed ratio λ and pitch angle β .

The mathematical models of a DFIG are essential requirement for its control system. The voltage equations of an induction motor in a rotating $d-q$ coordinate are as follows

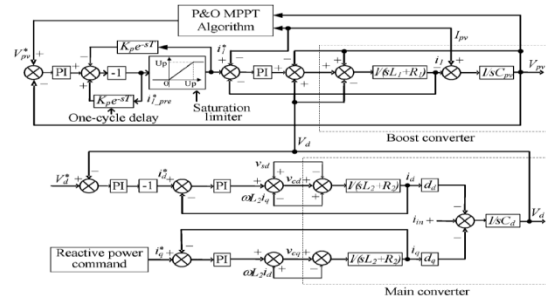


Fig. 5 The control block diagram for boost converter and main converter

$$\begin{bmatrix} u_{ds} \\ u_{qs} \\ u_{dr} \\ u_{qr} \end{bmatrix} = \begin{bmatrix} -R_s & 0 & 0 & 0 \\ 0 & -R_s & 0 & 0 \\ 0 & 0 & -R_r & 0 \\ 0 & 0 & 0 & -R_r \end{bmatrix} \begin{bmatrix} i_{ds} \\ i_{qs} \\ i_{dr} \\ i_{qr} \end{bmatrix} + p \begin{bmatrix} \lambda_{ds} \\ \lambda_{qs} \\ \lambda_{dr} \\ \lambda_{qr} \end{bmatrix}$$

$$+ \begin{bmatrix} -\omega_1 \lambda_{qs} \\ \omega_1 \lambda_{ds} \\ -\omega_2 \lambda_{qr} \\ \omega_2 \lambda_{dr} \end{bmatrix}$$

$$\begin{bmatrix} \lambda_{ds} \\ \lambda_{qs} \\ \lambda_{dr} \\ \lambda_{qr} \end{bmatrix} = \begin{bmatrix} -L_s & 0 & L_m & 0 \\ 0 & -L_s & 0 & L_m \\ -L_m & 0 & L_r & 0 \\ 0 & -L_m & 0 & L_r \end{bmatrix} \begin{bmatrix} i_{ds} \\ i_{qs} \\ i_{dr} \\ i_{qr} \end{bmatrix} \quad 7$$

The dynamic equation of the DFIG

$$\frac{J}{n_p} \frac{d\omega_r}{dt} = T_m - T_{em} \quad 8$$

$$T_{em} = n_p L_m (i_{qs} i_{dr}) \quad 9$$

Where the subscripts d, q, s , and denote d-axis, q-axis, stator, and rotor respectively, L represents the inductance, is the flux linkage, u and i represent voltage and current respectively, ω_1 and ω_2 are the angular synchronous speed and slip speed respectively, $\omega_2 = \omega_1 - \omega_r$, T_m is the mechanical torque, T_{em} is the electromagnetic torque and other parameters of DFIG are listed in Table 6.2. If the synchronous rotating - reference is oriented by the stator voltage vector, the $-$ axis is aligned with the stator voltage vector while the $-$ axis is aligned with

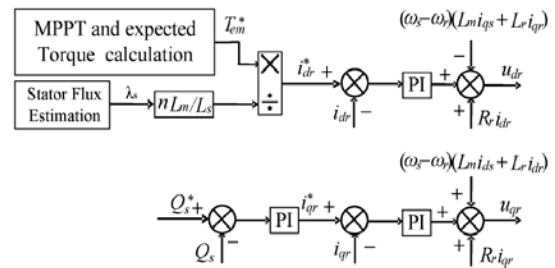


Fig. 6. The DTC control scheme for the rotor side converter.

the stator flux reference frame. Therefore, $\lambda_{ds}=0$ and $\lambda_{qs}=\lambda_s$. The following equations can be obtained in the stator voltage oriented reference frame as

$$i_{ds} = -\frac{L_m}{L_s} i_{dr}$$

$$T_{em} = n_p L_m \lambda_s i_{dr} \quad 10$$

$$\sigma = \frac{L_s L_r - L_m^2}{L_s L_r} \quad 11$$

$$v_{dr} = R_r i_{dr} + \sigma L_r \frac{di_{dr}}{dt} - (\omega_1 - \omega_r)(L_m i_{qs} + L_r i_{qr}) \quad 12$$

$$v_{qr} = R_r i_{qr} + \sigma L_r \frac{di_{qr}}{dt} - (\omega_1 - \omega_r)(L_m i_{ds} + L_r i_{dr}) \quad 13$$

3. COORDINATION CONTROL OF THE CONVERTERS

There are five types of converters in the hybrid grid. Those converters have to be coordinately controlled with the utility grid to supply an uninterrupted, high efficiency, and high quality power to variable dc and ac loads under variable solar irradiation and wind speed when the hybrid grid operates in both isolated and grid tied modes. The control algorithms for those converters are presented.

The control objectives for the converters change when the system transfers from one operating scenario to another.

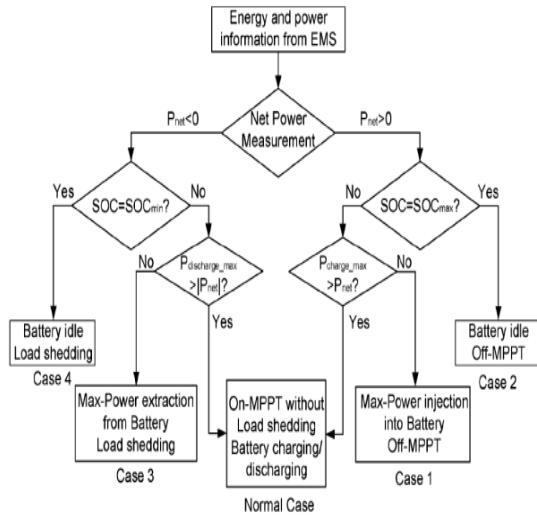


Fig.7 Control mode diagram for the isolated hybrid grid.

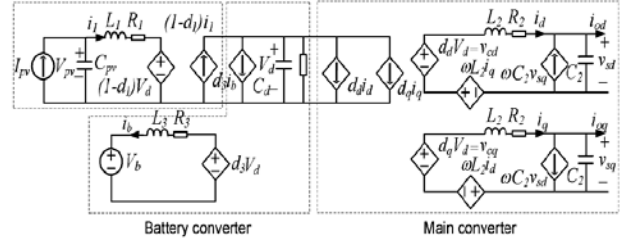


Fig. 8 Time average equivalent circuit model for the three converters

A Grid-Connected Mode

When the hybrid grid operates in this mode, the control objective of the boost converter is to track the MPPT of the PV array by regulating its terminal voltage. The back-to-back ac/dc/ac converter of the DFIG is controlled to regulate rotor side current to achieve MPPT and to synchronize with ac grid. The energy surplus of the hybrid grid can be sent to the utility system. The role of the battery as the energy storage becomes less important because the power is balanced by the utility grid. In this case, the only function of the battery is to eliminate frequent power transfer between the dc and ac link. The dc/dc converter of the battery can be controlled as the energy buffer using the technique. The main converter is designed to operate bidirectional to incorporate complementary characteristic of wind and solar sources. The control objectives of the main converter are to maintain a stable dc-link voltage for variable dc load and to synchronize with the ac link and utility system.

Power flow equations at the dc and ac links are as follows:

$$P_{pv} + P_{ac} = P_{acL} + P_b \quad 14$$

$$P_s = P_w - P_{acL} - P_{ac} \quad 15$$

Where real power P_{pv} and P_w are produced by PV and WTG respectively, P_{acL} and P_{dcL} are real power loads connected to ac and dc buses respectively, P_{ac} is the power exchange between ac and dc links, P_b is power injection to battery, and P_s is power injection from the hybrid grid or the utility. The current and voltage equations at dc bus are as follows

$$V_{pv} - V_T = L_1 \cdot \frac{di_1}{dt} + R_1 i_1 \quad 16$$

$$I_{pv} - i_1 = C_{pv} \cdot \frac{dV_{pv}}{dt} \quad 17$$

$$V_T = V_d \cdot (1 - d_1) \quad 18$$

$$i_1(1 - d_1) - C_d \frac{dV_d}{dt} - \frac{1}{R_L} V_d - i_b - i_{ac} = 0 \quad 19$$

Table 2 Parameters of doubly fed induction generator

Symbol	Description	Value
P_{nom}	Nominal power	50 kw
V_{nom}	Nominal voltage	400 V
R_s	Stator resistance	0.00706 pu
L_s	Stator inductance	0.171 pu
R_r	Rotor resistance	0.005 pu
L_r	Rotor inductance	0.156 pu
L_m	Mutual inductance	2.9 pu
J	Rotor inertia constant	3.1 s
n_p	Number of poles	6
$V_{dc,nom}$	Nominal DC voltage of AC/DC/AC converter	800 V
P_m	Nominal mechanical power	45 KW

The DFIG is controlled to maintain a stable dc-link voltage of the back-to-back ac/dc/ac converter. The objectives of the rotor side converter are to track MPPT of the WTG and to manage the stator side reactive power. Different control schemes such as the direct torque control (DTC) and direct power control (DPC) have been proposed for a DFIG. The DTC scheme as shown in Fig. 7.3 is selected as the control method for the rotor side converter in this project. The rotor rotational speed is obtained through the MPPT algorithm, which is based on the power and speed characteristic of the wind turbine. The rotational speed ω_r and mechanical power P_m are used to calculate the electromagnetic torque T_{em}^* .

The $-q$ axis rotor side current reference is determined based on T_{em}^* . Through stator flux estimation. The rotor side $d-q$ voltages are maintained through controlling the corresponding current with appropriate feed forward. When the hybrid grid operates in the islanding mode, the boost converter and the back-to-back ac/dc/ac converter of the DFIG may operate in the on-MPPT or off-MPPT based on system power balance and energy constraints. The dc-link voltage is maintained by either the battery or the boost converter based on system operating condition. Powers under various load and supply conditions should be balanced as follows

$$P_{pv} + P_w = P_{acL} + P_{dcL} + P_{Loss} + P_b \quad 22$$

Where P_{Loss} is the total grid loss.

Two level coordination controls are used to maintain system stable operation. At the system level, operation modes of the individual converters are determined by the energy management system (EMS) based on the system net power P_{net} and the energy constraints and the charging/discharging rate of battery.

The system control logic diagram is shown in Fig.7.4 P_{net} is defined as the total maximum power generation minus the total load and minus P_{loss} .

The energy constraints of the battery are determined based on the state of charge (SOC) limits using $SOC_{min} < SOC \leq SOC_{max}$. It should be noted that SOC cannot be measured directly, but can be attained through some estimation methods as described.

The constraint of charging and discharging rate is $P_b \leq P_{bmax}$. At local level, the individual converters operate based on mode commands from the EMS. Either the PV system or WTG or both have to operate in the off-MPPT mode for Case 1 and Case 2 and in the on-MPPT mode for other cases.

The time average equivalent circuit model of the booster, main converter, and battery converter for the isolated operation is shown in Fig. 8. The inverter part of the circuit model in Fig. 8 is based on the basic principles and descriptions. The current and voltage equations for the battery converter and dc link are as follows:

$$V_D - V_b = L_3 \cdot \frac{di_b}{dt} + R_3 i_b \quad 23$$

$$V_D = V_d \cdot d_3 \quad 24$$

$$i_1(1 - d_1) - i_{ac} - i_{dc} - i_b \cdot d_3 = i_c = C_d \cdot \frac{dV_d}{dt} \quad 25$$

Where d_3 and $(1 - d_3)$ are the duty ratio of the switches ST_7 and ST_8 respectively.

The ac side current equations of the main converter in $d-q$ coordinate are as follows

$$C_2 \frac{d}{dt} \begin{bmatrix} v_{sd} \\ v_{sq} \end{bmatrix} = \begin{bmatrix} i_d \\ i_q \end{bmatrix} + \begin{bmatrix} 0 & \omega \\ -\omega & 0 \end{bmatrix} \begin{bmatrix} v_{sd} \\ v_{sq} \end{bmatrix} - \begin{bmatrix} i_{od} \\ i_{oq} \end{bmatrix} \quad 26$$

Where i_{od} and i_{oq} are $d-q$ currents at the converter side of the transformer respectively.

Multi-loop voltage control for a dc/ac inverter is described, where the control objective is to provide a high quality ac voltage with good dynamic response at different load conditions. This control scheme can also be applied for main converter control to provide high quality ac voltage in stand-alone mode with minor modifications. The coordinated control block diagram for the normal case is shown in Fig. 9. To provide a stable dc-link voltage, the dual loop control scheme is applied for the battery converter. The injection current $i_{in} = (1 - d_1) - i_{ac} - i_{dc}$. It should be noted that the output of the outer voltage loop is multiplied by -1 before it is set as the inner loop current reference.

4. SIMULATION RESULTS

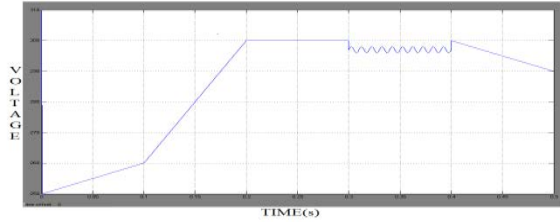


Fig.11 terminal voltage of solar panel

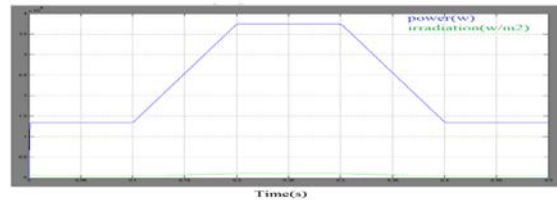


Fig.12 PV output power versus solar irradiation

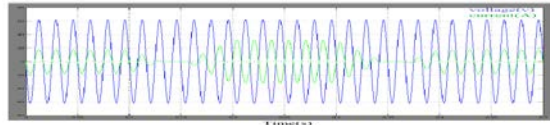


Fig.13 AC side voltage and current of the main converter with variable solar irradiation level and constant DC load

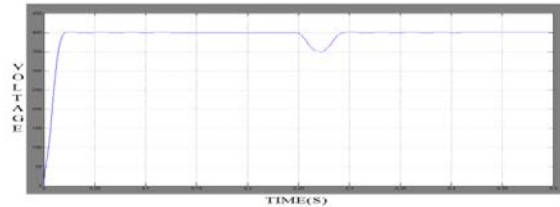


Fig.14 DC bus voltage transient response

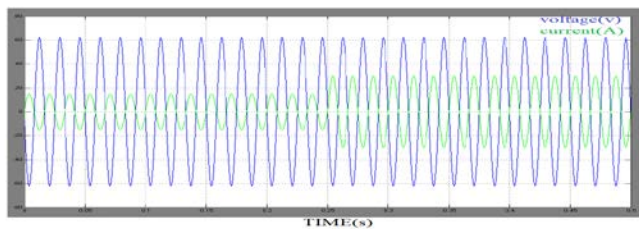


Fig.15 AC side voltage and current of the main converter with constant solar Irradiation level and variable dc load

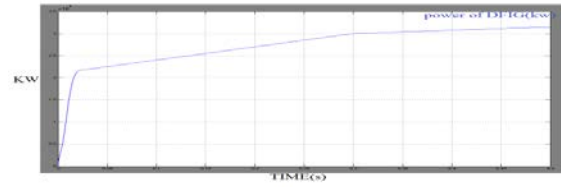


Fig.16 Output power of the doubly fed induction generator

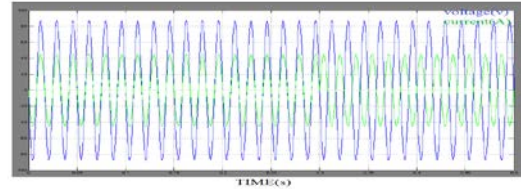


Fig.17 AC side voltage versus current

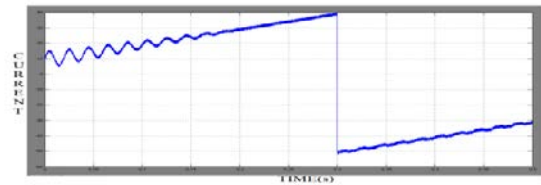


Fig.18 battery charging current

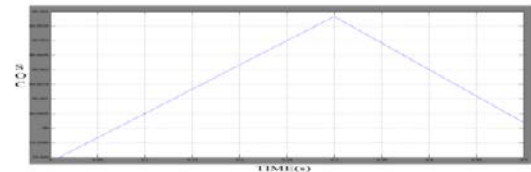


Fig.19 Battery state of charge

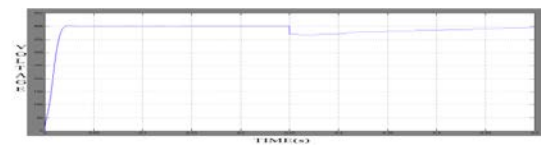


Fig.20 DC bus voltage transient response in isolated mode

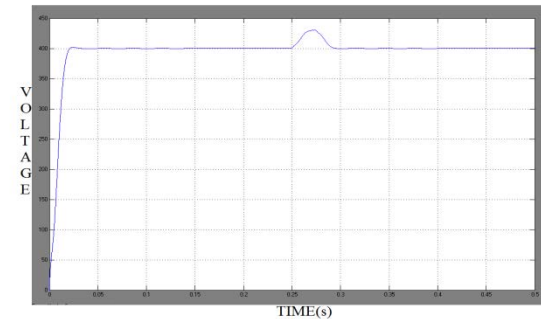


Fig.21 DC bus voltage

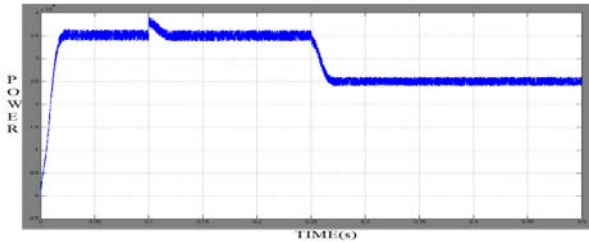


Fig.22 PV output power

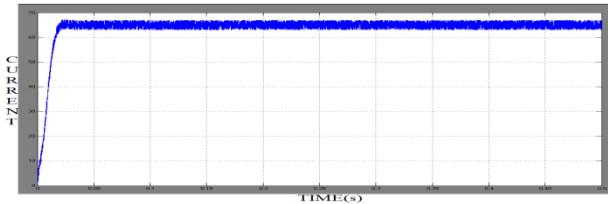


Fig.23 Battery current

CONCLUSION

A hybrid ac/dc micro grid is proposed and comprehensively studied in this project. The models and coordination control schemes are proposed for the all the converters to maintain stable system operation under various load and resource conditions. The coordinated control strategies are verified by MATLAB/Simulink. Various control methods have been incorporated to harness the maximum power from dc and ac sources and to coordinate the power exchange between dc and ac grid. Different resource conditions and load capacities are tested to validate the control methods. The simulation results show that the hybrid grid can operate stably in the grid-tied or isolated mode. Stable ac and dc bus voltage can be guaranteed when the operating conditions or load capacities change in the two modes. The power is smoothly transferred when load condition changes.

Although the hybrid grid can reduce the processes of dc/ac and ac/dc conversions in an individual ac or dc grid, there are many practical problems for implementing the hybrid grid based on the current ac dominated infrastructure. The total system efficiency depends on the reduction of conversion losses and the increase for an extra dc link. It is also difficult for companies to redesign their home and office products without the embedded ac/dc rectifiers although it is theoretically possible. Therefore, the hybrid grids may be implemented when some small customers want to install their own PV systems on the roofs and are willing to use LED lighting systems and EV charging systems. The hybrid grid may also be feasible for some small isolated industrial plants with both PV system and wind turbine generator as the major power supply.

REFERENCES

- [1] R. H. Lasseter, "Micro Grids," in Proc. IEEE Power Eng. Soc. Winter Meet., Jan. 2002, vol. 1, pp. 305–308.
- [2] Y. Zoka, H. Sasaki, N. Yorino, K. Kawahara, and C. C. Liu, "An interaction problem of distributed generators installed in a Micro Grid," in Proc. IEEE Elect. Utility Deregulation, Restructuring, Power Technol., Apr. 2004, vol. 2, pp. 795–799.
- [3] R. H. Lasseter and P. Paigi, "Micro grid: A conceptual solution," in Proc. IEEE 35th PESC, Jun. 2004, vol. 6, pp. 4285–4290.
- [4] C. K. Sao and P. W. Lehn, "Control and power management of converter fed Micro Grids," IEEE Trans. Power Syst., vol. 23, no. 3, pp. 1088–1098, Aug. 2008.
- [5] T. Logenthiran, D. Srinivasan, and D. Wong, "Multi-agent coordination for DER in Micro Grid," in Proc. IEEE Int. Conf. Sustainable Energy Technol., Nov. 2008, pp. 77–82.
- [6] M. E. Baran and N. R. Mahajan, "DC distribution for industrial systems: Opportunities and challenges," IEEE Trans. Ind. Appl., vol. 39, no. 6, pp. 1596–1601, Nov. 2003.
- [7] Y. Ito, Z. Yang, and H. Akagi, "DC micro-grid based distribution power generation system," in Proc. IEEE Int. Power Electron. Motion Control Conf., Aug. 2004, vol. 3, pp. 1740–1745.
- [8] A. Sannino, G. Postiglione, and M. H. J. Bollen, "Feasibility of a DC network for commercial facilities," IEEE Trans. Ind. Appl., vol. 39, no. 5, pp. 1409–1507, Sep. 2003.
- [9] D. J. Hammerstrom, "AC versus DC distribution systems—did we get it right?," in Proc. IEEE Power Eng. Soc. Gen. Meet., Jun. 2007, pp. 1–5.
- [10] D. Salomonsson and A. Sannino, "Low-voltage DC distribution system for commercial power systems with sensitive electronic loads," IEEE Trans. Power Del., vol. 22, no. 3, pp. 1620–1627, Jul. 2007.
- [11] M. E. Ropp and S. Gonzalez, "Development of a MATLAB/Simulink model of a single-phase grid-connected photovoltaic system," IEEE Trans. Energy Conv., vol. 24, no. 1, pp. 195–202, Mar. 2009.
- [12] K. H. Chao, C. J. Li, and S. H. Ho, "Modeling and fault simulation of photovoltaic generation systems using circuit-based model," in Proc. IEEE Int. Conf. Sustainable Energy Technol., Nov. 2008, pp. 290–294.
- [13] O. Tremblay, L. A. Dessaint, and A. I. Dekkiche, "A generic battery model for the dynamic simulation of hybrid electric vehicles," in Proc. IEEE Veh. Power Propulsion Conf. (VPPC 2007), pp. 284–289.
- [14] D. W. Zhi and L. Xu, "Direct power control of DFIG with constant switching frequency and improved transient performance," IEEE Trans. Energy Conv., vol. 22, no. 1, pp. 110–118, Mar. 2007.